

E-9705
6/19/95

Leading Edge Film Cooling Effects on Turbine Blade Heat Transfer

Vijay K. Garg
AYT Corporation
Brook Park, Ohio

and

Raymond E. Gaugler
Lewis Research Center
Cleveland, Ohio

Prepared for the
40th Gas Turbine and Aeroengine Congress and Exposition
sponsored by the American Society of Mechanical Engineers
Houston, Texas, June 5-8, 1995



National Aeronautics and
Space Administration

LEADING EDGE FILM COOLING EFFECTS ON TURBINE BLADE HEAT TRANSFER

Vijay K. Garg¹
AYT Corporation
Brookpark, OH

Raymond E. Gaugler¹
Turbomachinery Flow Physics Branch
Internal Fluid Mechanics Division
NASA Lewis Research Center
Mail Stop 5-11, Cleveland, OH

ABSTRACT

An existing three-dimensional Navier-Stokes code (Arnone et al., 1991), modified to include film cooling considerations (Garg and Gaugler, 1994), has been used to study the effect of spanwise pitch of shower-head holes and coolant to mainstream mass flow ratio on the adiabatic effectiveness and heat transfer coefficient on a film-cooled turbine vane. The mainstream is akin to that under real engine conditions with stagnation temperature = 1900 K and stagnation pressure = 3 MPa. It is found that with the coolant to mainstream mass flow ratio fixed, reducing P , the spanwise pitch for shower-head holes, from $7.5 d$ to $3.0 d$, where d is the hole diameter, increases the average effectiveness considerably over the blade surface. However, when $P/d = 7.5$, increasing the coolant mass flow increases the effectiveness on the pressure surface but reduces it on the suction surface due to coolant jet lift-off. For $P/d = 4.5$ or 3.0 , such an anomaly does not occur within the range of coolant to mainstream mass flow ratios analyzed. In all cases, adiabatic effectiveness and heat transfer coefficient are highly three-dimensional.

NOMENCLATURE

B_p blowing parameter $[= (\rho_c V_c) / \{\rho_o (RT_o)^{1/2}\}]$
 d coolant hole diameter
 h heat transfer coefficient based on $(T_o - T_w)$
 m mass flow rate
 p pressure
 P spanwise pitch of shower-head holes
 s distance from the leading edge along the pressure or suction surface
 S $= s/s_m$ on suction surface, and $= -s/s_m$ on pressure surface
 T temperature
 V_c average coolant velocity at the hole exit

y y -coordinate of the Cartesian coordinate system with origin at the geometric stagnation point
 y^+ dimensionless distance of the first point off the blade surface
 z z -coordinate along the span
 γ ratio of specific heats
 η adiabatic effectiveness $[= (T_o - T_{aw}) / (T_o - T_c)]$
 ρ density

Subscripts

aw corresponding to adiabatic condition
 c for coolant (average value)
 e freestream (external) value
 m maximum value
 n corresponding to uncooled blade
 o stagnation value
 w at the blade surface

1. INTRODUCTION

The search for better performance of gas turbine engines has led to higher turbine inlet temperatures. Modern gas turbine engines are designed to operate at inlet temperatures of 1800-2000 K, which are far beyond the allowable metal temperatures. Under these conditions, the turbine blades need to be cooled in order to ensure a reasonable lifetime. This calls for an efficient cooling system. Discrete jet film cooling is one of the techniques used to protect the blades and endwalls that are thermally exposed. Since the injected cooler air is bled directly from the compressor before it passes through the combustion chamber, the best compromise between admissible metal temperature and aerodynamic efficiency becomes a major objective in cooled turbine blade design.

A considerable effort has been devoted into understanding the

¹Fellow ASME

coolant film behavior and its interaction with the mainstream flow. The film cooling performance is influenced by the wall curvature, three-dimensional external flow structure, free-stream turbulence, compressibility, flow unsteadiness, the hole size, shape and location, and the angle of injection. Many studies on film cooling have been confined to simple geometries, for example, two-dimensional flat and curved plates in steady, incompressible flow. An excellent survey of the work up to 1971 has been provided by Goldstein (1971). While several further studies in this field have been summarized by Garg and Gaugler (1993, 1994), some recent ones are discussed here.

Bons et al. (1994) investigated the effect of high freestream turbulence (up to 17%) on the adiabatic effectiveness of a single row of film cooling holes injecting into a turbulent, zero pressure gradient boundary layer on a flat plate. Their experiments show that elevated levels of free stream turbulence reduce film cooling effectiveness by up to 70% in the region directly downstream of the injection hole due to enhanced mixing, while they produce a 50-100% increase in effectiveness in the region between injection holes. The latter is due to accelerated spanwise diffusion of the cooling fluid, which also produces an earlier merger of the coolant jets from adjacent holes. However, their study does not include the effects of such additional factors as turbulent length scales, streamwise pressure gradient, curvature, multiple rows of holes, density ratio, etc. In fact, the coolant to freestream density ratio was held constant at about 0.95 while typical values in a gas turbine engine application vary from 1.5 to 2.0.

Lee et al. (1994) investigated the effect of free-stream turbulence (up to 8%), blowing ratio (0.5 and 1.0) and injection location (40, 50 and 60 degrees from the front stagnation point) on the mass transfer in the vicinity of an injection hole normal to a cylindrical surface, using a naphthalene sublimation technique. When the coolant is injected at 40°, the mass transfer upstream of the jet is not affected by the coolant jet at all. However, when the injection hole is located beyond 50° the mass transfer upstream of the jet suddenly increases due to the formation of a horseshoe vortex, but it decreases as the free-stream turbulence increases because of a weaker horseshoe vortex structure. While the circular cylindrical surface was used to simulate the leading edge of a turbine blade, the shower-head holes are compound-angled unlike the radially injecting holes in these experiments.

Jabbari et al. (1994) measured the effectiveness for injection through discrete holes in the endwall of a turbine blade for three blowing rates, two density ratios, and two approaching Reynolds numbers, using a mass transfer technique described by Goldstein (1971) in a low-speed wind tunnel with a planar cascade. They found that even sixty locations are insufficient for describing the strong local variations in the effectiveness values. Their work provides qualitative information revealing the paths and interaction of the jets that change with blowing rate and density ratio.

In companion studies, Sen et al. (1994) and Schmidt et al. (1994) measured heat transfer coefficients and film cooling effectiveness for compound angle injection from a single row of holes in a flat plate test facility with zero pressure gradient. Round holes and holes with a diffusing expanded exit were used. While experiments for film cooling effectiveness were performed

at a density ratio of 1.6, those for heat transfer coefficient measurement were performed at a density ratio of 1.0. It was found that the compound angle holes with an expanded exit had a much improved lateral distribution of coolant near the hole for all momentum flux ratios. All hole geometries had similar maximum spatially averaged effectiveness at a low momentum flux ratio of 0.25. Although compound angle holes with an expanded exit had significantly improved adiabatic effectiveness at high momentum flux ratio, these holes were found to have poorer overall performance when combined with heat transfer results. Thus, the importance of knowing both adiabatic effectiveness and heat transfer coefficient for evaluating overall film cooling performance, specially for compound angle injection at high momentum flux ratios, was clearly brought out by these companion studies.

In a memorial tribute, Kim et al. (1994) presented a summary of the cooled turbine blade tip heat transfer and film effectiveness studies by the late Professor Metzger along with recent experimental data for various combinations of clearance heights, clearance flow Reynolds numbers, and film flow rates with different coolant injection configurations. For the case of film injection at the blade-tip pressure side corner, the average film cooling effectiveness downstream of injection was found to increase with injection rate, whereas the same is not necessarily true for the airfoil pressure side injection. Results for the grooved-tip cavity injection indicate that overall film cooling performance varies significantly with injection locations. For a given film-to-mainstream mass flow ratio, the discrete slot injection is found to provide a superior film protection over other types of injections studied.

Hay et al. (1994) measured the coefficient of discharge of 30° inclined holes having a length to diameter ratio of 6, and rounded entries or exits, for a range of crossflow conditions. The rounding radius varied from 0 to 1 hole diameter, and the crossflow Mach number from 0 to 0.5. In the absence of crossflow, inlet rounding increased the discharge coefficient by as much as 30%. Rounding the hole inlet was also found to increase the discharge coefficient by up to 15% at high coolant (inlet) side crossflow Mach numbers. Rounding the exit, however, produced no significant benefit. The crossflow effects were correlated using inlet and outlet additive loss coefficients, and the correlation predicted the discharge coefficient well. However, for a smaller length to diameter ratios used in turbine blades, significant residual inlet flow distortions will be present at the hole outlet, thereby impairing the accuracy of prediction by the correlation. Moreover, in many gas turbine applications, much higher Mach numbers and coolant to mainstream density ratios are encountered than those used in the experiments of Hay et al. (1994).

Fougeres and Heider (1994) solved the unsteady three-dimensional Navier-Stokes equations, completed by a mixing-length turbulence model, using a finite volume technique. They presented two applications of the multi-domain code; one for a single row of hot jets injected into a flat plate turbulent boundary layer, and another for a plane nozzle guide vane with two rows of staggered holes on the pressure as well as suction side of the vane. The injection holes were discretized on cylindrical subdomains overlapping the mesh for the main flow. Comparison

with experimental data for the span-averaged heat transfer coefficient on the vane surface is qualitative in certain regions. The authors attributed some of this disagreement to insufficient mesh refinement but they also note that the code is very sensitive to the mesh characteristics, and that orthogonality of the near wall mesh is absolutely necessary.

Weigand and Harasgama (1994) carried out a numerical investigation of film cooling on a turbine rotor blade using Dawes (1993) code that utilizes an unstructured solution adaptive grid methodology for solving three-dimensional Navier-Stokes equations. The code uses a low Reynolds number $k-\epsilon$ model for turbulence. The authors considered a uniform as well as a non-uniform radial temperature distribution (RTD) at inlet to the rotating blade. However, a rather academic case of blowing in tangential direction was studied due to limitations of the code. As such, comparison with experimental data was not possible. They considered two blowing geometries; one with a single slot located at mid-span and two single holes near the hub and the tip of the blade, and another with two rows of staggered slots (total three) at mid-span and two rows of staggered holes (total six) near the hub and the tip of the blade. After a converged solution with a total mass error smaller than 1% was obtained on a coarse grid with about 73000 tetrahedral cells and about 15000 nodes, the grid was carefully refined to a total of about 358000 cells associated with about 67000 nodes. It was found that blowing on the pressure side of the blade resulted in some of the coolant flow being transported through the tip gap of the blade to the suction side. Also, the effect of RTD on the film cooling effectiveness is most significant near the tip of the blade. At the hub and near mid-span of the blade the film cooling effectiveness distributions are very similar with or without RTD.

Hall et al. (1994) analyzed the shower-head film cooling on the C3X vane with a multi-block, three-dimensional Navier-Stokes code using the Baldwin-Lomax turbulence model. Taking advantage of the spanwise periodicity of the planar C3X vane, the computational span was restricted to just one spanwise pitch of the shower-head holes. The final airfoil C-grid had over 2.1 million grid points with a 17×17 grid patch on each of the five holes. Such a grid refinement cannot be handled by present day computers if the vane were annular requiring the whole span to be analyzed, not just a slice of it. The computational domain included the film cooling holes but not the plenum chamber. Hall et al. (1994) carried out a grid-dependence study much like the one carried out by Garg and Gaugler (1993) for the C3X vane with four rows of gill holes. The term, gill holes, denotes the location of holes on a blade similar to that of gills on a fish. They recommend that a minimum y^+ value of 3.0 or less be maintained for the near airfoil mesh to achieve accurate heat transfer results, while Boyle and Giel (1992) recommended a value of y^+ about 1. They observed adjacent jet merging and a pronounced "stripping" pattern on the suction surface at low coolant flow rates, but at high coolant rates, the film-cooling flow followed a more spanwise trajectory resulting in a more uniform reduction in heat transfer at the vane surface.

Garg and Gaugler (1994) modified the three-dimensional Navier-Stokes code of Arnone et al. (1991) to include the capability of analyzing heat transfer on a film-cooled blade. They

did not discretize the hole pipe but applied appropriate boundary conditions at the hole exit on the blade surface, representing each hole exit by several control volumes (about 20). They analyzed the C3X vane with nine rows of film cooling holes, and found a fair comparison with the near mid-span experimental data of Hylton et al. (1988). Their computations show a strong spanwise variation of the heat transfer coefficient on the blade surface, specially with shower-head cooling, while almost all experimental data is near mid-span or span-averaged.

Liu et al. (1994) implemented a bulk film cooling capability in a three-dimensional viscous code with the Baldwin-Lomax turbulence model to recognize the global effect of mass, momentum and energy addition without attempting to resolve the details of the cooling air jet and its mixing evolution with the main flow. Using this code, the first stage of a gas producer turbine was designed, and cases with and without cooling were compared. Overall, the stator contained 34 rows of cooling holes, with 5 rows on the showerhead, 3 gill rows on the suction side, 2 gill rows on the pressure side, 3 rows on the pressure side at mid-chord, 4 axial rows approximating the trailing edge slots on the pressure surface just upstream of the trailing edge, 9 rows on the shroud endwall, and 8 rows of holes on the hub endwall. The sheared H-grid used had only 218530 points. Results were provided for pressure and temperature distribution but not for heat transfer coefficient involving temperature gradient at the surface, due perhaps to a lack of enough resolution.

The above survey indicates that while experimental effort in film cooling is shifting toward the real geometry, there is still a considerable effort devoted to flat plate studies with somewhat unrealistic parameters such as the length to diameter ratio, the density ratio, etc. On the other hand, the computational effort is almost solely devoted to the real blade, though still stationary except for the analysis of Weigand and Harasgama (1994). Also, while the analysis of Liu et al. (1994) forms one extreme in that no resolution of the mixing of coolant with the main flow was attempted, the analysis of Weigand and Harasgama (1994) and of Leylek and Zerkle (1994) represents the other extreme with the hole pipe and plenum chamber also discretized. Both these extremes have merits and limitations. While the poor resolution of Liu et al. (1994) perhaps prevented them from presenting any heat transfer results, they could consider the whole vane along with the hub and shroud endwalls containing 34 rows with hundreds of film cooling holes. On the other hand, Leylek and Zerkle analyzed just one row of holes on a flat plate (just one hole for computational purposes), while Weigand and Harasgama (1994) considered a total of nine holes in two rows on a rotating blade but with (unrealistic) injection in the tangential direction. While Leylek and Zerkle's approach is good to resolve the near-hole and within-hole physics, it cannot be extended to a real blade with hundreds of holes, at least with present-day computers. It can be used to feed the hole-exit information into a "middle-of-the-road" approach taken by Garg and Gaugler (1994), wherein appropriate boundary conditions are imposed at the hole exits on the blade surface instead of resolving the coolant flow within the hole pipe. Garg and Gaugler's analysis provides proper resolution for accurate prediction of surface heat transfer coefficients, and is still computationally manageable for analyzing the whole blade

with hundreds of holes. For example, Garg and Gaugler's computational span was about 20% of the total span for the C3X vane with nine rows of holes. They used about one million grid points with 30 holes in the computational domain.

Herein, we follow the analysis of Garg and Gaugler (1994) in order to study the effect of spanwise pitch of shower-head holes, and coolant to mainstream mass flow ratio on the adiabatic effectiveness and heat transfer coefficient on the film-cooled C3X vane with nine rows of film cooling holes including five rows on the shower-head.

2. ANALYSIS

The three-dimensional Navier-Stokes code of Arnone et al. (1991) for the analysis of turbomachinery flows was modified by Garg and Gaugler (1994) to include film cooling effects. Briefly, the code is an explicit, multigrid, cell-centered, finite volume code with an algebraic turbulence model. The Navier-Stokes equations in a rotating Cartesian coordinate system are mapped onto a general body-fitted coordinate system using standard techniques. Viscous effects in the streamwise direction are neglected in comparison to those in the other two directions. Justification for this assumption is provided in Garg and Gaugler (1994). The multistage Runge-Kutta scheme developed by Jameson et al. (1981) is used to advance the flow solution in time from an initial guess to the steady state. A spatially varying time step along with a CFL number of 5 was used to speed convergence to the steady state. Eigenvalue-scaled artificial dissipation and variable-coefficient implicit residual smoothing are used along with a full-multigrid method.

The effects of film cooling have been incorporated into the code in the form of appropriate boundary conditions at the hole locations on the blade surface. Each hole exit is represented by several control volumes (about 20) having a total area equal to the area of the hole exit, and passing the same coolant mass flow. Different velocity and temperature profiles for the injected gas can be specified at the hole exit. For the cases reported here, turbulent (1/7th power-law) for the coolant velocity and temperature profiles at the hole exit were specified, in conformity with the observation of Leyeck and Zerkle (1994), since the hole-length to diameter ratio for the C3X vane is 3.4. Leyeck and Zerkle (1994) found that for high hole-length to diameter ratios (≥ 3.0) and high blowing ratios (≥ 1.0), the velocity profile at the hole exit is akin to the 1/7th power-law profile. These profiles also yield better comparison with the experimental data for the C3X vane than the polynomial profiles at the hole exit (Garg and Gaugler, 1995).

For computation of the adiabatic effectiveness, the blade surface was considered adiabatic while for computation of the heat transfer coefficient at the blade surface, it was considered isothermal. The algebraic mixing length turbulence model of Baldwin and Lomax (1978) was used. This model was designed for the prediction of wall bounded turbulent shear layers, and may not be appropriate for flows with massive separations or large vortical structures. Thus, this model is likely to be invalid in a number of turbomachinery applications but for turbine blades, the boundary layers generally experience a favorable pressure gradient whereby this model is more likely to be valid. It has been used

satisfactorily by Boyle and Giel (1992), Ameri and Arnone (1994a, b), and Boyle and Ameri (1994) for heat transfer calculations on turbine blades without film cooling, and by Hall et al. (1994), and Garg and Gaugler (1994) with film cooling. In fact, Ameri and Arnone (1994b) compared the Baldwin-Lomax model and Coakley's $q-\omega$ model against experimental data of Graziani et al. (1980), and found that the algebraic model was able to produce many of the flow features better than the two-equation model. They further state that this conclusion is strengthened when one takes into account the relative economy of computations with the algebraic model. It is known (Amer et al., 1992) that two-equation models are also not satisfactory in the presence of film cooling. Perhaps the multiple-time-scale turbulence model of Kim and Benson (1992) may be more appropriate. However, use of this model is computationally very expensive since it involves solving four more partial differential equations in addition to the five at present, all coupled.

3. C3X VANE

Figure 1 shows the C3X vane with the film cooling hole details, as tested by Hylton et al. (1988). The test vane was internally cooled by an array of ten radial cooling holes (not shown in Fig. 1) in the active part of the vane. In addition to the details available in Fig. 1, the two rows of holes on the pressure surface were located at $s/s_m = 0.197, 0.225$, and on the suction surface at $s/s_m = 0.254, 0.276$. One row of shower-head holes was located at the geometric leading edge, with one row on the suction side and three on the pressure side. While other details of the vane geometry were held fixed, the spanwise pitch of shower-head holes was varied in the present investigation from the original 7.5 d to 3.0 d, in order to study its effect on the heat transfer coefficient and effectiveness over the vane surface.

4. COMPUTATIONAL DETAILS

The computational span, shown in Fig. 2, is only a part of the real span. The ordinate in Fig. 2 denotes the distance along the blade surface in the spanwise direction, while the abscissa denotes the distance along the blade surface in the streamwise direction, both normalized by the hole radius, r . It may be noted that the abscissa in Fig. 2 has breaks so as to accommodate all the rows of holes. The shape and orientation of the hole openings in Fig. 2 is a direct consequence of the angles the holes make with the spanwise or streamwise direction. The pattern of holes shown in Fig. 2 is repeated in the spanwise direction. Periodic boundary conditions are imposed due to shower-head injection on the ends of the computational span, which shrinks as the spanwise pitch of shower-head holes is reduced. Moreover, for spanwise pitch of shower-head holes = 7.5d and 4.5d (Figs. 2a and 2b), the computational span equals twice the spanwise pitch, while for the pitch of 3d (Fig. 2c), it is only one spanwise pitch.

Since the hole diameter is about 1 mm, the grid size has to be varied along the blade chord. For computational accuracy, the ratio of two adjacent grid sizes in any direction was kept within 0.76 to 1.3. A periodic C-grid with up to one million grid points was used. Depending upon the spanwise pitch of shower-head holes, the grid used was $281 \times 45 \times 81$ or $281 \times 45 \times 49$ or $281 \times 45 \times 17$ where the first number represents the number of grid points along

the main flow direction, the second in the blade-to-blade direction, and the third in the span direction. Grids for all three cases of spanwise pitch of shower-head holes were the same; the lower number of grid points in the span direction for lower values of spanwise pitch corresponds exactly to the extent of computational span for the case (cf. Fig. 2). Normal to the blade surface is the dense viscous grid, with $y^+ < 1$ for the first point off the blade surface, following Boyle and Giel (1992). Computations were run on the 8-processor Cray Y-MP supercomputer at the NASA Lewis Research Center, and on the 16-processor C-90 supercomputer at NASA Ames Research Center. The code requires about 60 million words (Mw) of storage and takes about 20 s per iteration (full-multigrid) on the C-90 machine for one million grid points. For a given grid the first isothermal blade case requires about 1100 iterations to converge, while subsequent cases (corresponding to different values of the parameters) for the same grid require about 300 iterations starting with the solution for the previous case. For an adiabatic blade surface, the number of iterations required is at least twice that for an isothermal blade.

5. RESULTS AND DISCUSSION

Results were obtained for air ($\gamma = 1.4$) with inlet total pressure, $p_0 = 3$ MPa, inlet total temperature, $T_0 = 1900$ K, exit Mach number ≈ 0.87 , and exit Reynolds number based on the axial chord $\approx 3.4 \times 10^6$. The coolant temperature, T_c , was taken to be half of T_0 (so that the density ratio is about two), while the blowing parameter, B_p , was varied so that the ratio of coolant mass flow to inlet mass flow changed from about 2% to 7%. For the case of $P/d = 7.5$, B_p was specified the same value for all holes. When the spanwise pitch of shower-head holes = 4.5 d or 3.0 d, the value of B_p for the shower-head holes was reduced in direct proportion to the spanwise pitch in order to keep the ratio of coolant mass flow to inlet mass flow the same as for the case of $P/d = 7.5$. We may point out that for film cooling on a turbine vane or blade, it is better to use the blowing parameter than the usual blowing ratio since the latter is based on the local free-stream velocity and density that change all over the airfoil. For injection at the stagnation line, for example, the blowing ratio is infinite, while the blowing parameter is finite. The term "blowing ratio" perhaps originated with fundamental studies of a jet in crossflow for which the blowing ratio is akin to the blowing parameter. In the following, we discuss results for the adiabatic effectiveness and heat transfer coefficient separately. Values are actually provided for h/h_n , where h_n is the heat transfer coefficient with no film cooling. The net benefit from film cooling can be quantified by $(1 - h/h_n)$.

5.1 Adiabatic Effectiveness

Figure 3 displays the blade-surface-area-averaged effectiveness values over the pressure and suction surfaces of the C3X vane, while Fig. 4 displays the same for the entire C3X vane surface as a function of the ratio of coolant to inlet mass flow. Clearly, the average effectiveness increases with m_c/m_0 for all cases except on the suction surface when $P/d = 7.5$. From Fig. 3, it is clear that the average η on the suction surface increases considerably as P/d decreases. However, on the pressure surface the average η is about the same for $P/d = 4.5$ or 3.0. For the entire blade, Fig. 4,

the average effectiveness increases with increasing coolant flow and decreasing P/d ratio.

Figures 5 to 7 show the adiabatic effectiveness contours over the C3X vane for spanwise pitch of shower-head holes = 7.5 d, 4.5 d and 3.0 d, respectively. In each figure, results are provided for four values of the coolant to inlet mass flow ratio. The effectiveness contours are given at intervals of 0.1, and clearly exhibit strong streamwise as well as spanwise variation. We may point out that while the abscissa represents about 128 mm of streamwise distance on the C3X vane in Figs. 5 to 7, the ordinate represents only about 15, 9 and 3 mm of the computational span in Figs. 5, 6 and 7, respectively. For the sake of clarity, the abscissa in these figures covers only 40% of the blade surface on either side of the stagnation line. Over about 10 - 20% of chord downstream of the gill holes, the effectiveness values exhibit a wavelike behavior with higher values directly downstream of holes and lower values between the holes. From Fig. 5, it is clear that the effectiveness is low in the region between the shower-head holes and gill holes on the suction side, and, in fact, it reduces with increasing m_c/m_0 ratio, contrary to the expectation. We will discuss the reason for this behavior later. On the pressure side, the effectiveness values do increase with increasing coolant flow in all cases. On the suction side, however, η decreases with increasing coolant flow for the spanwise pitch of shower-head holes = 7.5 d in Fig. 5, while the reverse is true for the results in Figs. 6 and 7. Comparing Figs. 5, 6 and 7, we find that, in general, the effectiveness increases with decreasing spanwise pitch to diameter ratio for the shower-head holes.

The evidence for decreasing effectiveness values on the suction surface with increasing coolant flow when $P/d = 7.5$ is provided by the static temperature ratio (T/T_0) contours in Fig. 8. The ratio of coolant to inlet mass flow for this figure is 0.0355. The north-east portion of this figure shows the C3X vane with nine rows of holes located by black lines, and two more locations (where temperature contours are displayed) shown in green. A blow-up of the front part of the vane is also shown. The temperature contours in the y - z plane are shown at four streamwise locations represented by different values of the index i . While $i = 117$ and $i = 149$ represent the shower-head hole spanwise centerlines on the pressure and suction side, respectively, $i = 111$ and $i = 158$ represent locations about 3.5 d and 7.5 d downstream, respectively, of the closest hole. It is clear from the contours at $i = 158$ that hot gas from the freestream has migrated to the vane surface due to lift off of the coolant jet from the vane surface. The coolant jet is thus no longer effective in cooling the surface. This is due to the secondary flow within the coolant jet, and the resulting entrainment of the hot gas from the outer region towards the airfoil surface between the adjacent jets. The lift-off is a jet-crossflow interaction based upon pressure fields and momentum balances (Haas et al., 1991). The penetration of the coolant jet from the shower-head holes depends mainly on the injection angle, on the momentum ratio $(\rho_c V_c^2)/(\rho_e V_e^2)$, and on the pitch-to-diameter ratio P/d . While the injection angle was kept constant, the other two parameters were varied in the present study.

Though not shown here, it was found that the hot gas entrainment increased resulting in more rapid lift off of the coolant jet downstream of the shower-head hole ($i = 149$ location)

on the suction side as the coolant flow rate was increased when $P/d = 7.5$. Obviously, an increase in the coolant flow rate corresponds to an increase in the coolant momentum as well. This explains why the effectiveness decreases on the suction surface with an increase in coolant flow rate when $P/d = 7.5$. On the pressure surface, $i = 111$, the coolant shower-head jet does not lift off the surface, thus resulting in higher effectiveness values than those on the suction surface. Another reason for higher effectiveness values on the pressure surface is the closer proximity of the shower-head holes to gill holes on the pressure side in comparison to that on the suction side.

Similar to Fig. 8, Figs. 9 and 10 show the static temperature ratio contours in the y - z plane for $m_c/m_o = 0.0355$ when $P/d = 4.5$ and 3.0, respectively. The same four i locations are chosen for comparing the results in Figs. 8 to 10. It is clear from Fig. 9 that when P/d is reduced to 4.5, the coolant jet does not lift off the suction surface though the hot fluid does penetrate to cover a part of the airfoil surface between the holes. This is due to the closer proximity of the coolant jets to each other when $P/d = 4.5$ than that when $P/d = 7.5$ (Fig. 8). When $P/d = 3.0$, the hot fluid is unable to reach the vane surface between the holes (Fig. 10), and thus the coolant is effective over the entire span. On the pressure surface, the hot fluid is unable to reach the airfoil surface for $P/d = 4.5$ or 3.0 (see Fig. 9 or 10, $i = 111$) leading to high adiabatic effectiveness values that are little different from each other whether $P/d = 4.5$ or 3.0.

5.2 Heat Transfer Coefficient

For computing the heat transfer coefficient, the vane surface temperature was taken to be $0.7 T_o$. Also, with no film cooling, h_n is independent of the spanwise location, thus requiring just one run of the code. Actually, the code is three-dimensional while for the linear cascade vane such as the C3X vane, we need to run only a two-dimensional version of the code to compute h_n . Figures 11 to 13 show the contours for h/h_n at intervals of 0.1 for the four values of m_c/m_o for each of $P/d = 7.5, 4.5$ and 3.0, respectively. We may point out that the ordinate in these figures is stretched in exactly the same manner as in Figs. 5 to 7. Since $(1 - h/h_n)$ represents the net benefit from film cooling, values of h/h_n closer to zero are desirable. Presence of negative values of h/h_n at some locations simply implies that the direction of heat transfer is reversed at these locations due to specification of the isothermal wall boundary condition ($T_w/T_o = 0.7$ here) and coolant temperature ($T_c = 0.5 T_o$ here). From these figures, we observe that the heat transfer coefficient, like the adiabatic effectiveness, is a strong function of the streamwise as well as spanwise location. Unfortunately, most experimental data available to date does not provide the spanwise variation since it is either span-averaged (based on, sometimes, as few as just two spanwise measurements) or near mid-span, as is true of the experimental data on the C3X vane (Hylton et al., 1988).

Similar to the results for adiabatic effectiveness in Figs. 5 to 7, we observe a wavelike structure of the heat transfer coefficient in Figs. 11 to 13 over about 10 - 20% of chord downstream of the gill holes, with lower values directly downstream of the gill holes and higher values between the holes. From Fig. 11, we observe that values of h/h_n are high (and thus net benefit from film

cooling is low) on the suction surface, and increase with the coolant mass flow. This is again due to the coolant jet lifting off the airfoil surface for this case, as explained earlier via Fig. 8. On the pressure surface, values of h/h_n are fairly low (or even negative) for all cases except when $m_c/m_o = 0.0211$. Thus, the pressure surface is fairly well cooled. Reducing the value of P/d from 7.5 to 3.0 helps greatly in providing better film cooling benefit on the suction surface. On the pressure surface, however, there is little gain in reducing P/d from 4.5 to 3.0.

6. CONCLUSIONS

It is found that with the coolant to mainstream mass flow ratio fixed, reducing the spanwise pitch for shower-head holes from 7.5 d to 3.0 d increases the average adiabatic effectiveness considerably over the blade surface. However, when $P/d = 7.5$ for the C3X vane, increasing the coolant mass flow reduces the adiabatic effectiveness on the suction surface due to coolant jet lifting off the vane surface - a consequence of the secondary flow within the coolant jet and its interaction with the hot surrounding fluid. For $P/d = 4.5$ or 3.0, such an anomaly does not occur within the range of coolant to mainstream mass flow ratios studied. In all cases, adiabatic effectiveness and heat transfer coefficient are highly three-dimensional.

ACKNOWLEDGEMENTS

This work was done when the first author held a National Research Council - NASA Research Associateship at the NASA Lewis Research Center. Helpful discussions with A.A. Ameri and R.J. Boyle of the NASA Lewis Research Center are gratefully acknowledged.

REFERENCES

- Amer, A.A., Jubran, B.A. and Hamdan, M.A., 1992, "Comparison of Different Two-Equation Turbulence Models for Prediction of Film Cooling from Two Rows of Holes," *Numer. Heat Transfer*, Vol. 21, Part A, pp. 143-162.
- Ameri, A.A. and Arnone, A., 1994a, "Transition Modeling Effects on Turbine Rotor Blade Heat Transfer Predictions," ASME Paper 94-GT-22.
- Ameri, A.A. and Arnone, A., 1994b, "Prediction of Turbine Blade Passage Heat Transfer Using a Zero and a Two-Equation Turbulence Model," ASME Paper 94-GT-122.
- Arnone, A., Liou, M.-S. and Povinelli, L.A., 1991, "Multigrid Calculation of Three-Dimensional Viscous Cascade Flows," AIAA Paper 91-3238.
- Baldwin, B.S. and Lomax, H., 1978, "Thin-Layer Approximation and Algebraic Model for Separated Turbulent Flows," AIAA Paper 78-257.
- Bons, J.P., MacArthur, C.D. and Rivir, R.B., 1994, "The Effect of High Freestream Turbulence on Film Cooling Effectiveness," ASME Paper 94-GT-51.
- Boyle, R.J. and Ameri, A.A., 1994, "Grid Orthogonality Effects on Predicted Turbine Midspan Heat Transfer and Performance," ASME Paper 94-GT-123.
- Boyle, R.J. and Giel, P., 1992, "Three-Dimensional Navier Stokes Heat Transfer Predictions for Turbine Blade Rows," AIAA Paper 92-3068.

Dawes, W.N., 1993, "The Extension of a Solution-Adaptive Three-Dimensional Navier-Stokes Solver Toward Geometries of Arbitrary Complexity," *J. Turbomachinery*, Vol. 115, pp. 283-295.

Fougeres, J.M. and Heider, R., 1994, "Three-Dimensional Navier-Stokes Prediction of Heat Transfer with Film Cooling," ASME Paper 94-GT-14.

Garg, V.K. and Gaugler, R.E., 1993, "Heat Transfer in Film-Cooled Turbine Blades," ASME Paper 93-GT-81.

Garg, V.K. and Gaugler, R.E., 1994, "Prediction of Film Cooling on Gas Turbine Airfoils," ASME Paper 94-GT-16.

Garg, V.K. and Gaugler, R.E., 1995, "Effect of Velocity and Temperature Distribution at the Hole Exit on Film Cooling of Turbine Blades," ASME Paper 95-GT-2.

Goldstein, R.J., 1971, "Film Cooling," *Advances in Heat Transfer*, Vol. 7, pp. 321-379.

Graziani, R.A., Blair, M.F., Taylor, J.R. and Mayle, R.E., 1980, "An Experimental Study of Endwall and Airfoil Surface Heat Transfer in a Large Scale Turbine Blade Cascade," *J. Eng. Power*, Vol. 102, pp. 257-267.

Haas, W., Rodi, W. and Schönung, B., 1991, "The Influence of Density Difference Between Hot and Coolant Gas on Film Cooling by a Row of Holes: Predictions and Experiments," ASME Paper 91-GT-255.

Hall, E.J., Topp, D.A. and Delaney, R.A., 1994, "Aerodynamic/Heat Transfer Analysis of Discrete Site Film-Cooled Turbine Airfoils," AIAA Paper 94-3070.

Hay, N., Lampard, D. and Khaldi, A., 1994, "The Coefficient of Discharge of 30° Inclined Film Cooling Holes with Rounded Entries or Exits," ASME Paper 94-GT-180.

Hylton, L.D., Nirmalan, V., Sultanian, B.K. and Kaufman, R.M., 1988, "The Effects of Leading Edge and Downstream Film Cooling on Turbine Vane Heat Transfer," NASA CR 182133.

Jabbari, M.Y., Marston, K.C., Eckert, E.R.G. and Goldstein, R.J., 1994, "Film Cooling of the Gas Turbine Endwall by Discrete-Hole Injection," ASME Paper 94-GT-67.

Jameson, A., Schmidt, W. and Turkel, E., 1981, "Numerical Solutions of the Euler Equations by Finite Volume Methods Using Runge-Kutta Time-Stepping Schemes," AIAA Paper 81-1259.

Kim, S.-W. and Benson, T.J., 1992, "Calculation of a Circular Jet in Cross Flow with a Multiple-Time-Scale Turbulence Model," *Intl. J. Heat Mass Transfer*, Vol. 35, pp. 2357-2365.

Kim, Y.W., Abdel-Messeh, W., Downs, J.P., Soechting, F.O., Steuber, G.D. and Tanrikut, S., 1994, "A Summary of the Cooled Turbine Blade Tip Heat Transfer and Film Effectiveness Investigations Performed by Dr. D.E. Metzger," ASME Paper 94-GT-167.

Lee, J.S., Ro, S.T. and Seo, H.J., 1994, "Mass Transfer Effects of Free-Stream Turbulence and Horseshoe Vortex Formed at the Upstream Edge of Film Cooling Jets about a Cylindrical Surface," ASME Paper 94-GT-18.

Leylek, J.H. and Zerkle, R.D., 1994, "Discrete-Jet Film Cooling: A Comparison of Computational Results With Experiments," *J. Turbomachinery*, Vol. 116, pp. 358-368.

Liu, J.S., Utz, R. and Bozzola, R., 1994, "Aerodynamic Design and Analysis of a Gas Producer Turbine Stator with Film Cooling Injection," AIAA Paper 94-2928.

Schmidt, D.L., Sen, B. and Bogard, D.G., 1994, "Film Cooling with Compound Angle Holes: Adiabatic Effectiveness," ASME Paper 94-GT-312.

Sen, B., Schmidt, D.L. and Bogard, D.G., 1994, "Film Cooling with Compound Angle Holes: Heat Transfer," ASME Paper 94-GT-311.

Weigand, B. and Harasgama, S.P., 1994, "Computations of a Film Cooled Turbine Rotor Blade with Non-Uniform Inlet Temperature Distribution Using a Three-Dimensional Viscous Procedure," ASME Paper 94-GT-15.

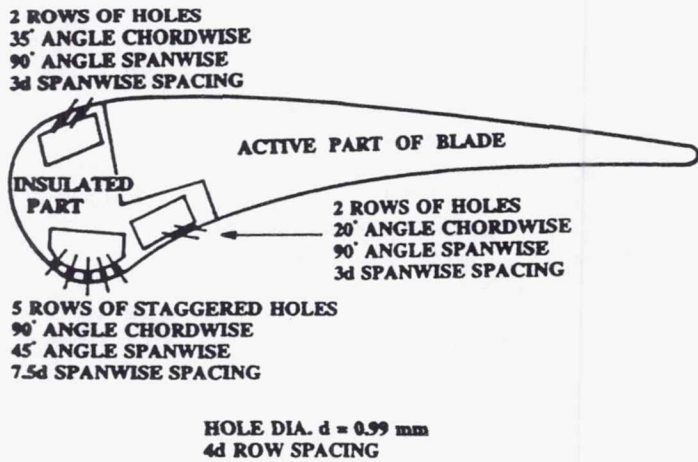


FIG. 1 C3X VANE AND COOLING HOLE DETAILS.

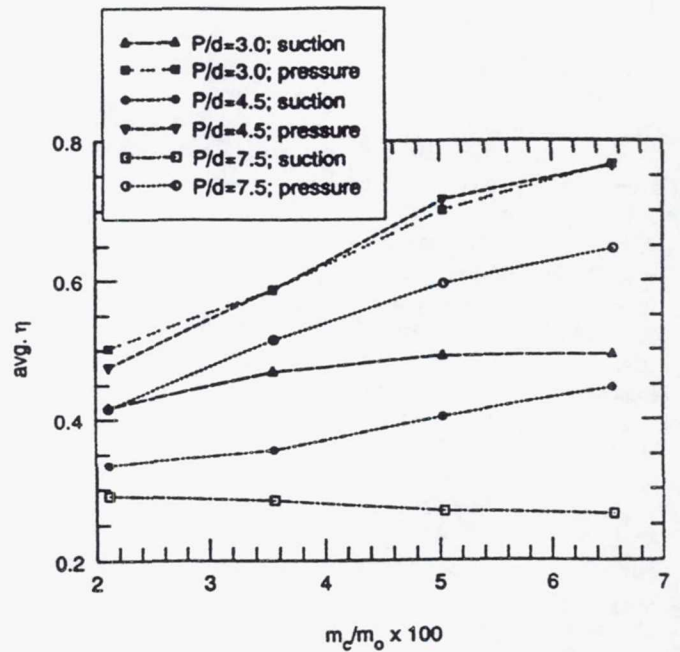


FIG. 3 AVERAGE EFFECTIVENESS ON THE PRESSURE AND SUCTION SURFACES AS A FUNCTION OF m_c/m_o .

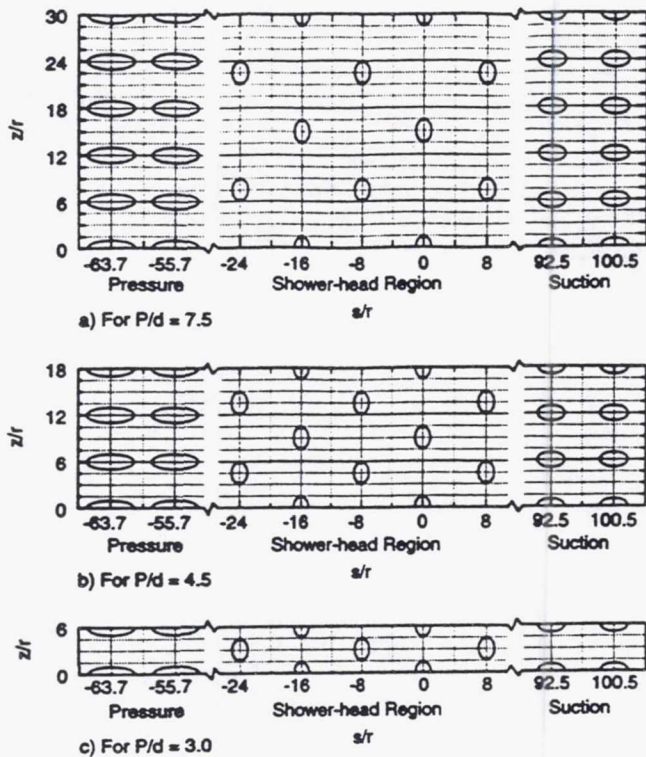


FIG. 2 COMPUTATIONAL SPAN FOR THE C3X VANE.

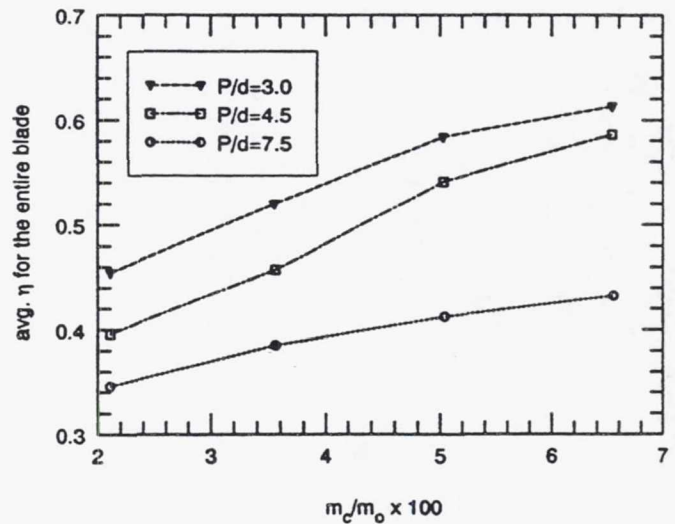


FIG. 4 AVERAGE EFFECTIVENESS ON THE ENTIRE C3X VANE SURFACE AS A FUNCTION OF m_c/m_o .

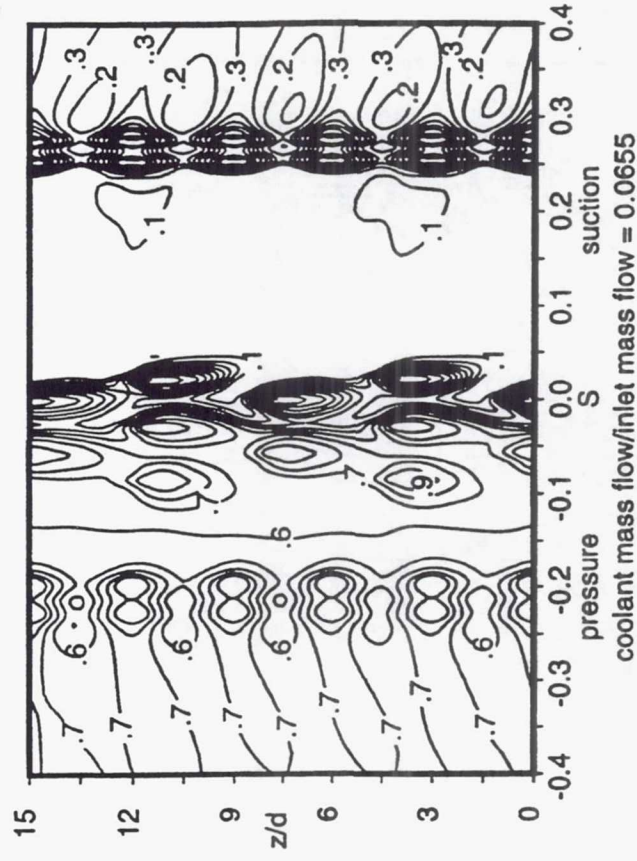
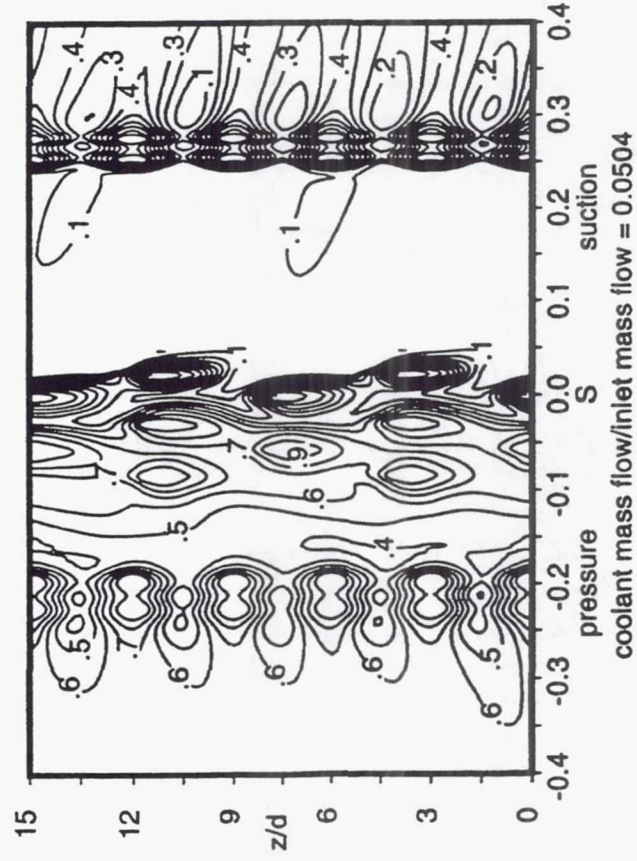
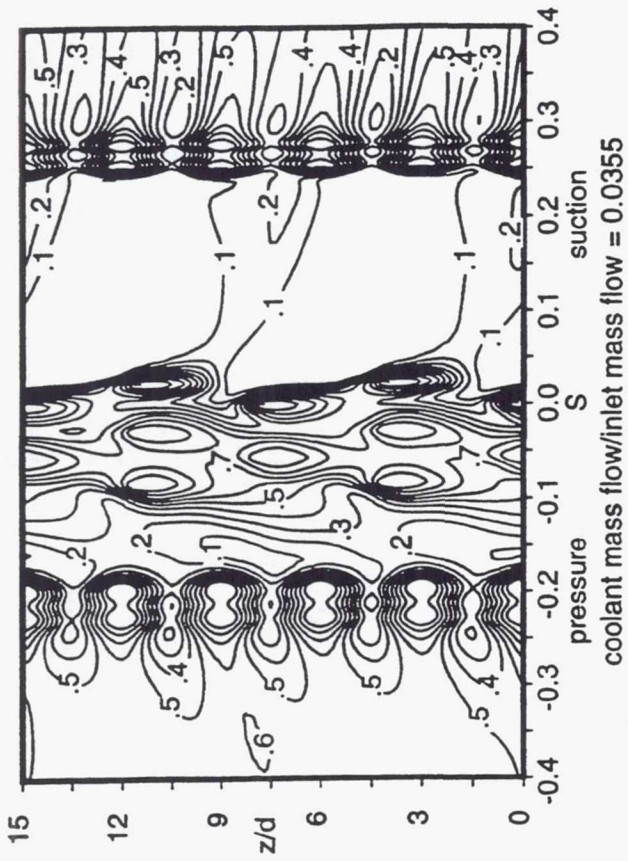
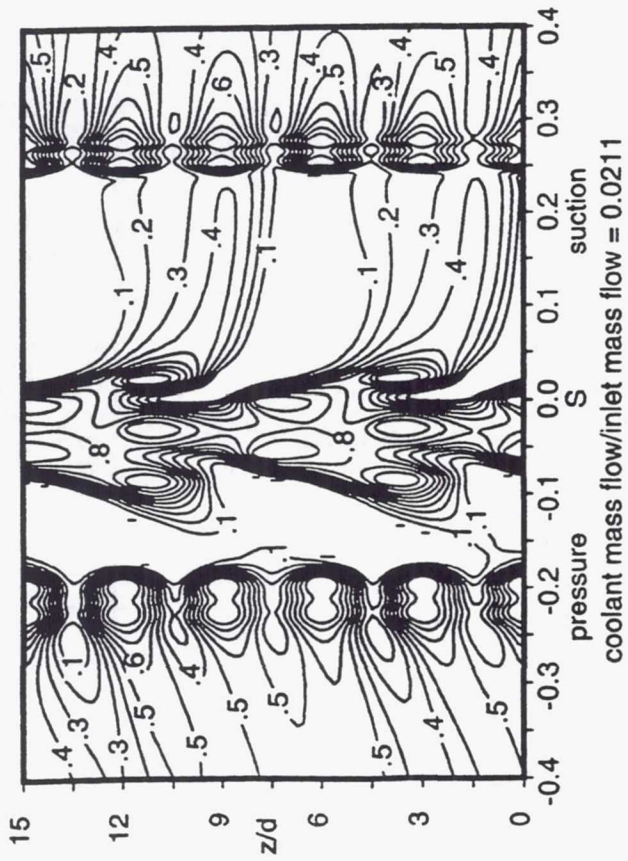


FIG. 5 ADIABATIC EFFECTIVENESS CONTOURS ON THE C3X VANE SURFACE WHEN $P/d = 7.5$.

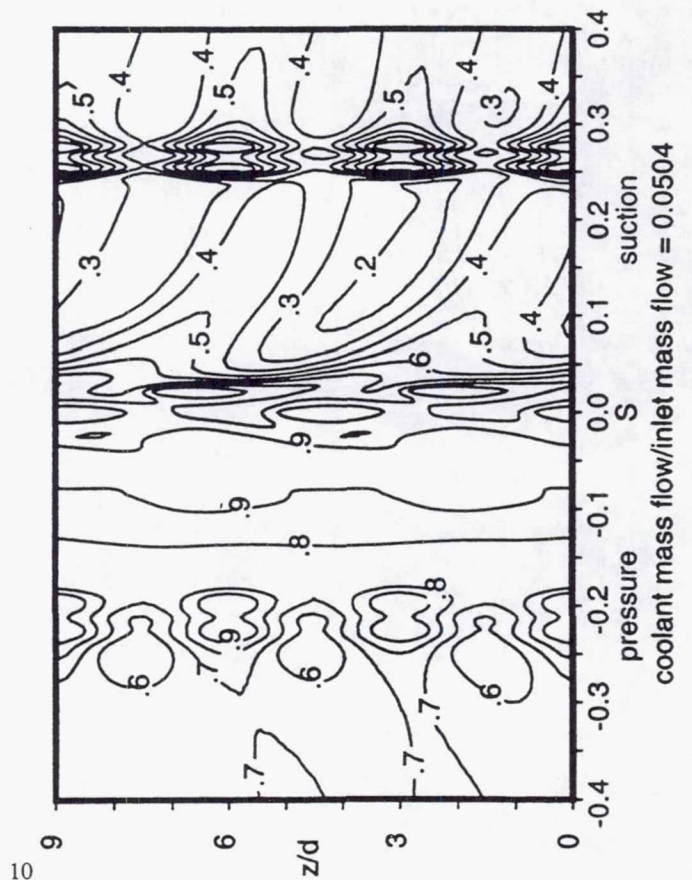
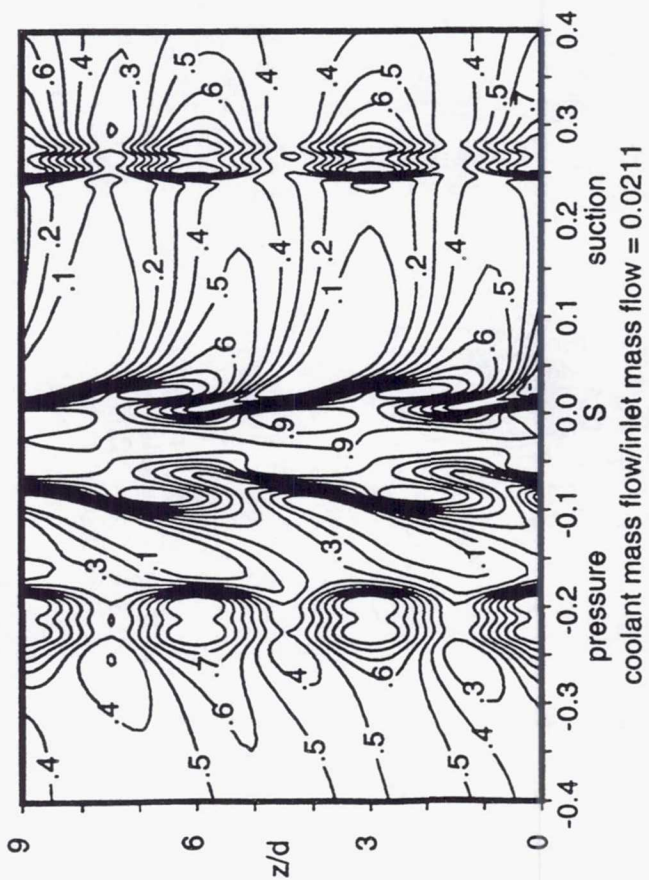
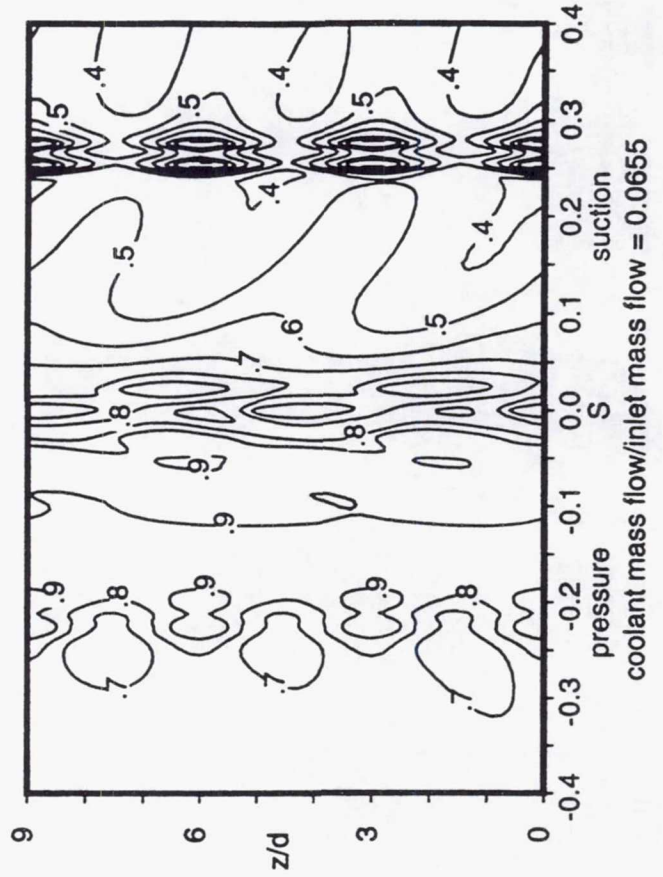
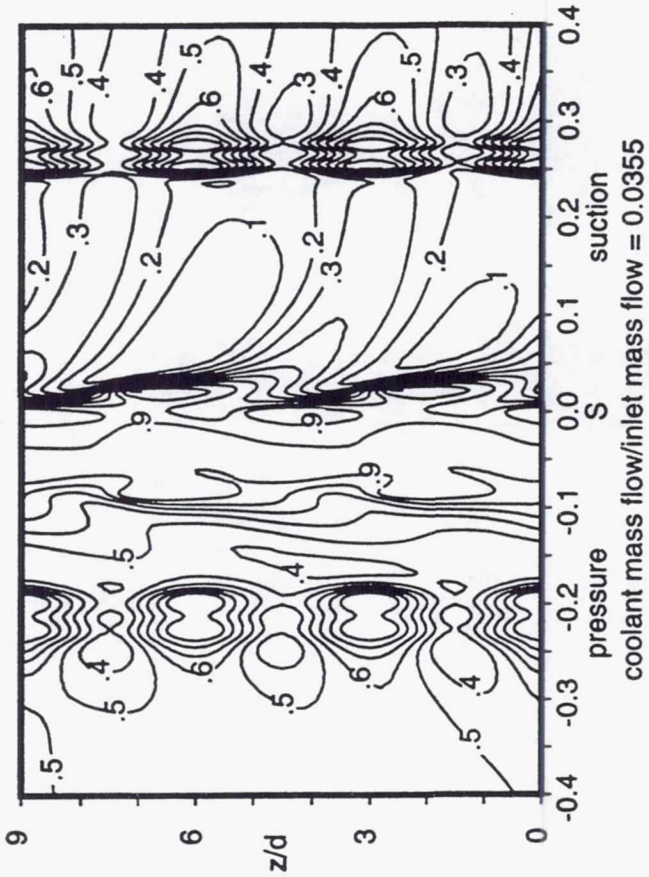


FIG. 6 ADIABATIC EFFECTIVENESS CONTOURS ON THE C3X VANE SURFACE WHEN $P/d = 4.5$.

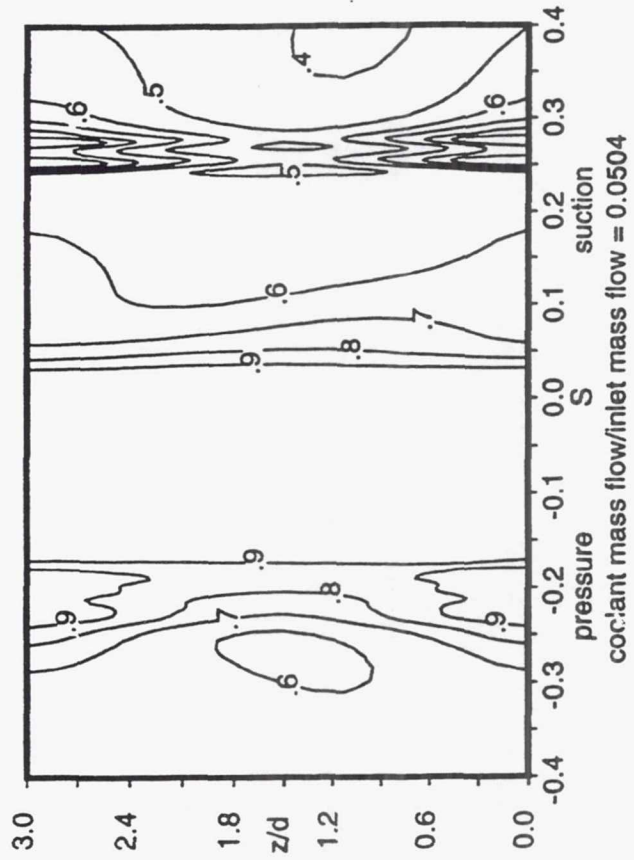
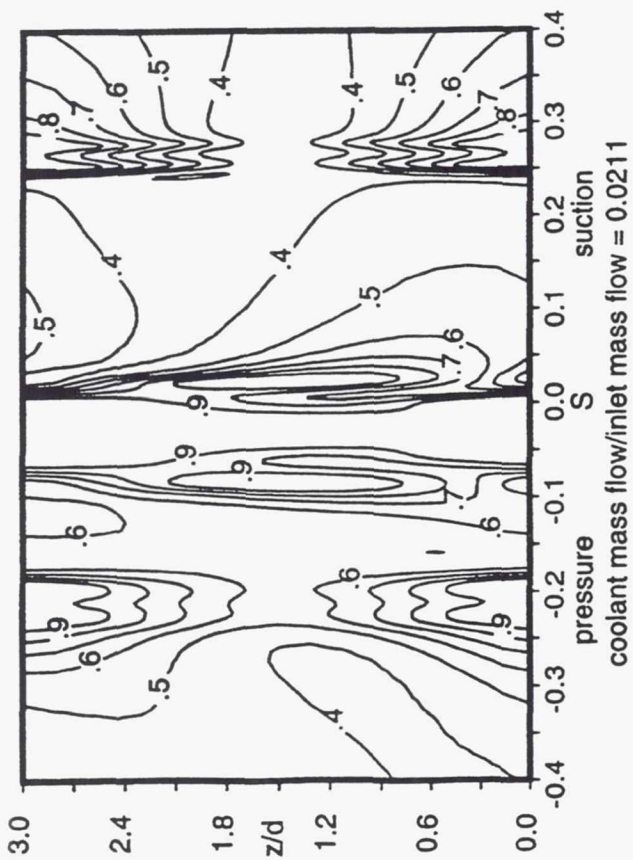
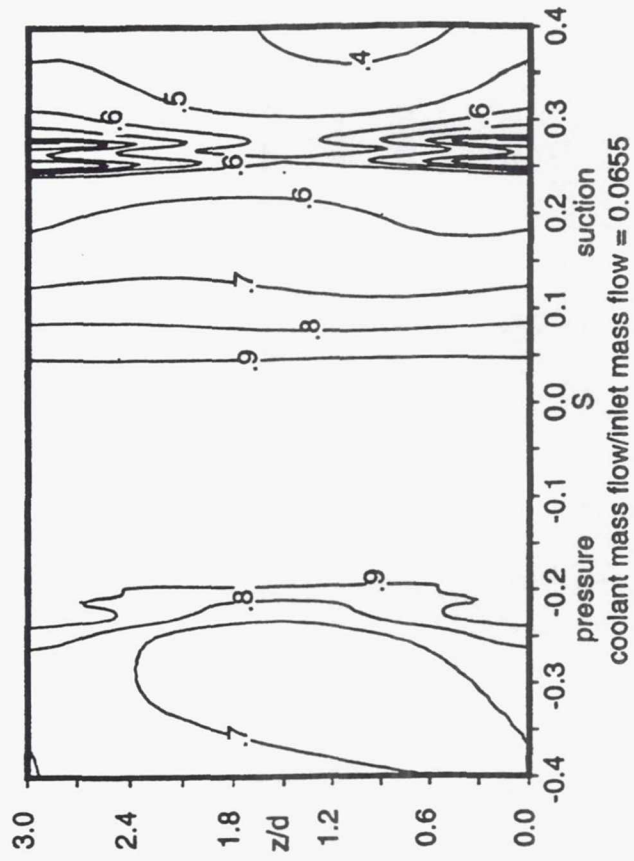
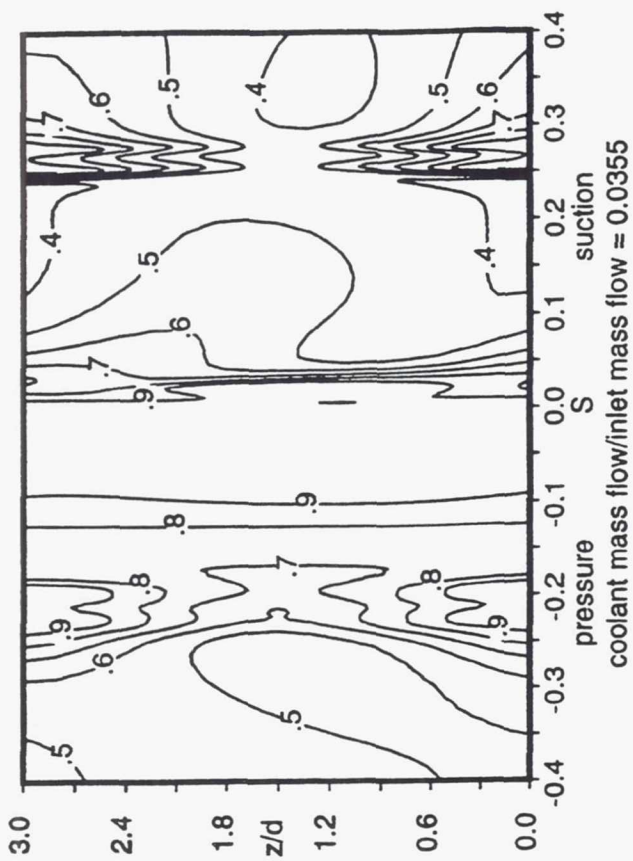


FIG. 7 ADIABATIC EFFECTIVENESS CONTOURS ON THE C3X VANE SURFACE WHEN $P/d = 3.0$.

Page intentionally left blank

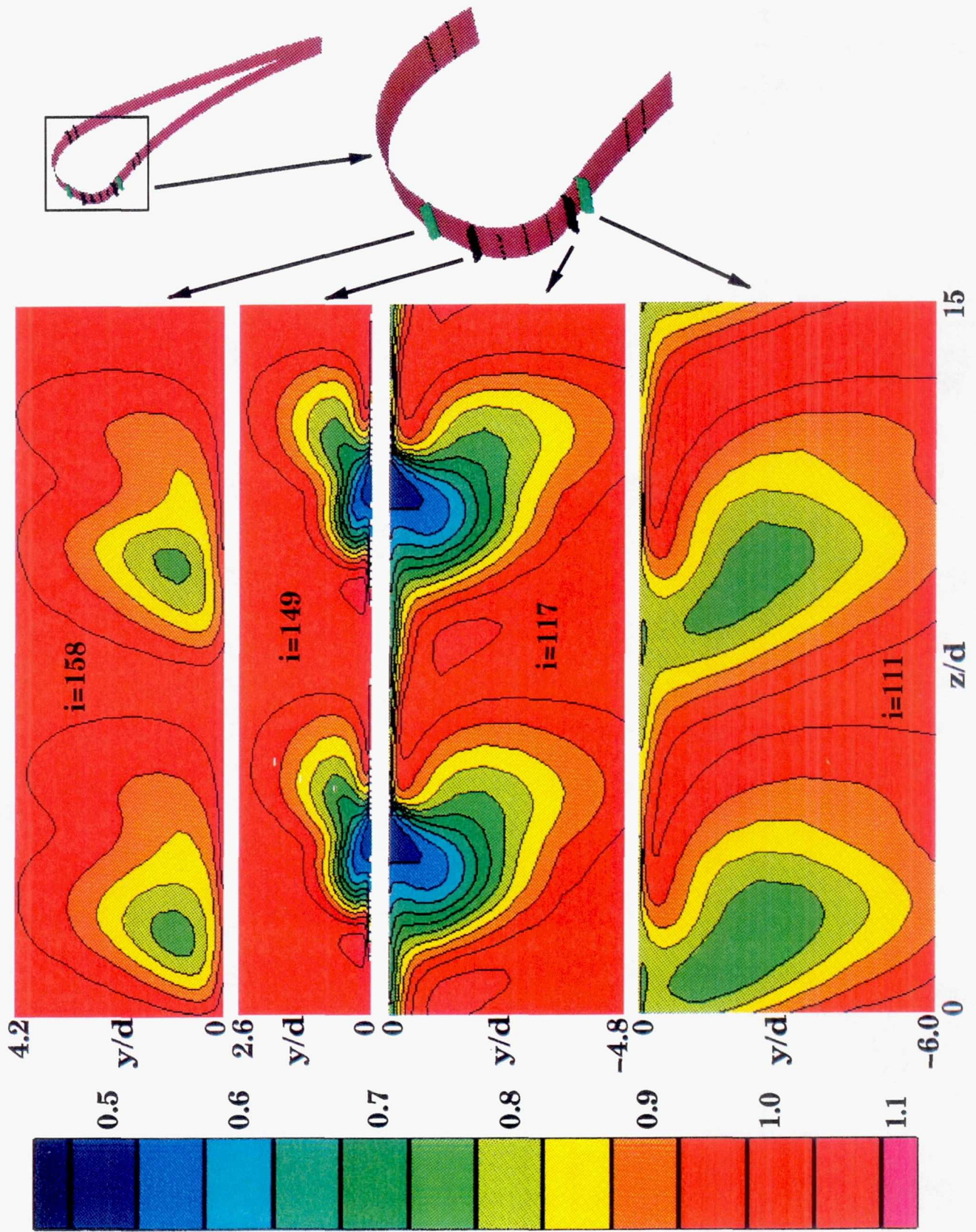


FIG. 8 STATIC TEMPERATURE RATIO CONTOURS AT SOME STREAMWISE LOCATIONS WHEN $P/d = 7.5$; $m_c/m_o = 0.0355$

Page intentionally left blank

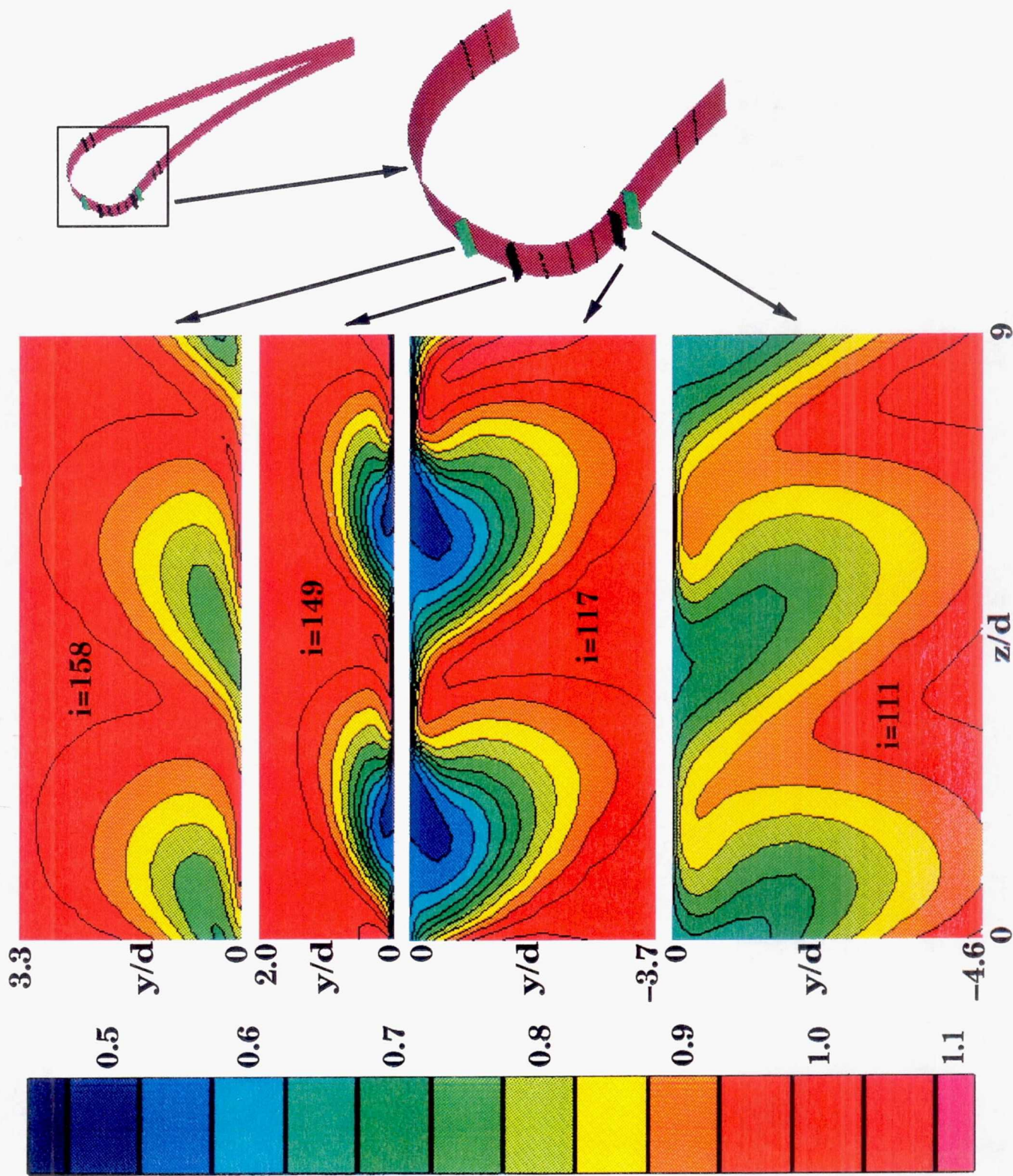


FIG. 9 STATIC TEMPERATURE RATIO CONTOURS AT SOME STREAMWISE LOCATIONS WHEN $P/d = 4.5$; $m_c/m_o = 0.0355$

Page intentionally left blank

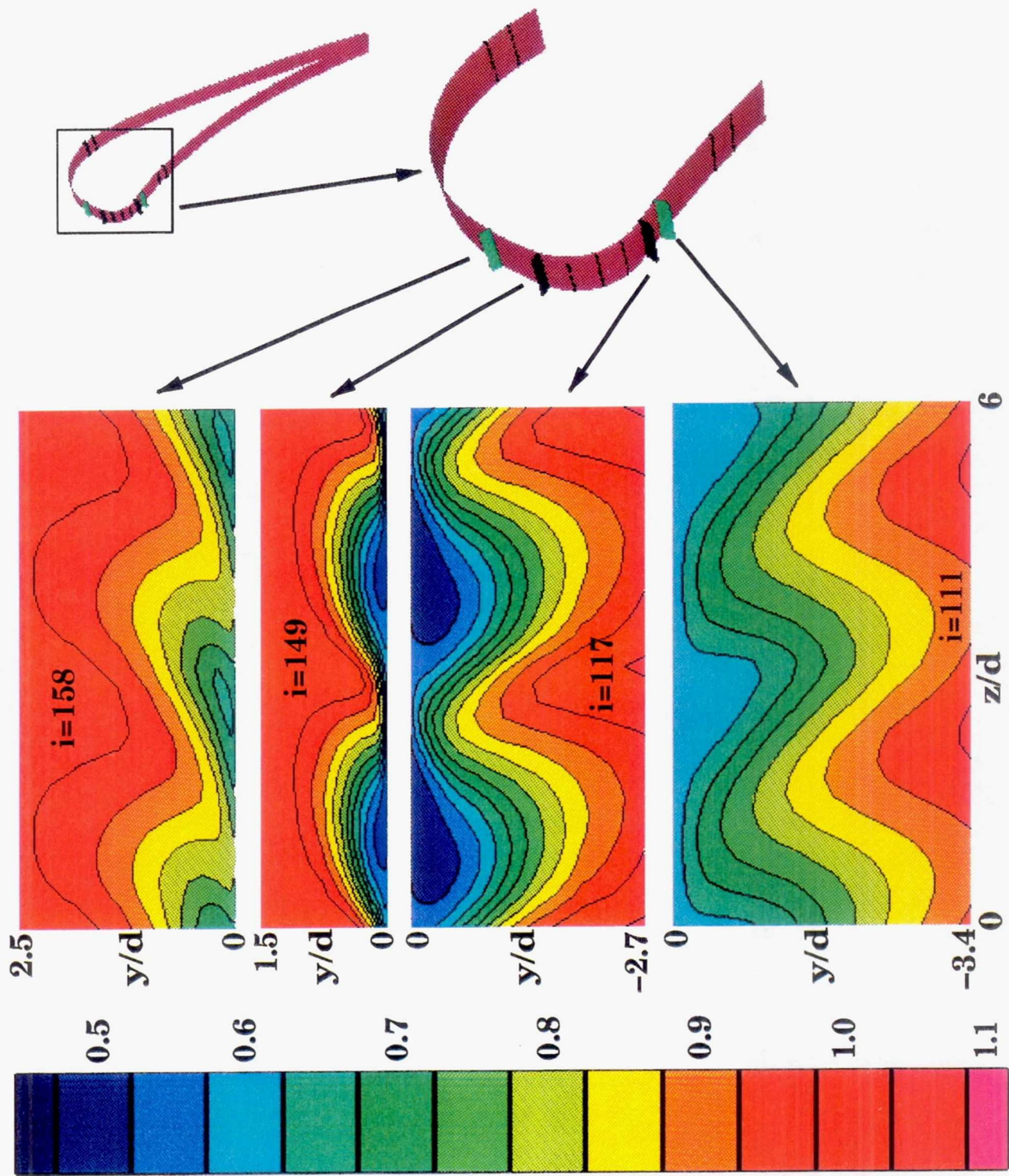


FIG. 10 STATIC TEMPERATURE RATIO CONTOURS AT SOME STREAMWISE LOCATIONS WHEN $P/d = 3.0$; $m_c/m_o = 0.0355$

Page intentionally left blank

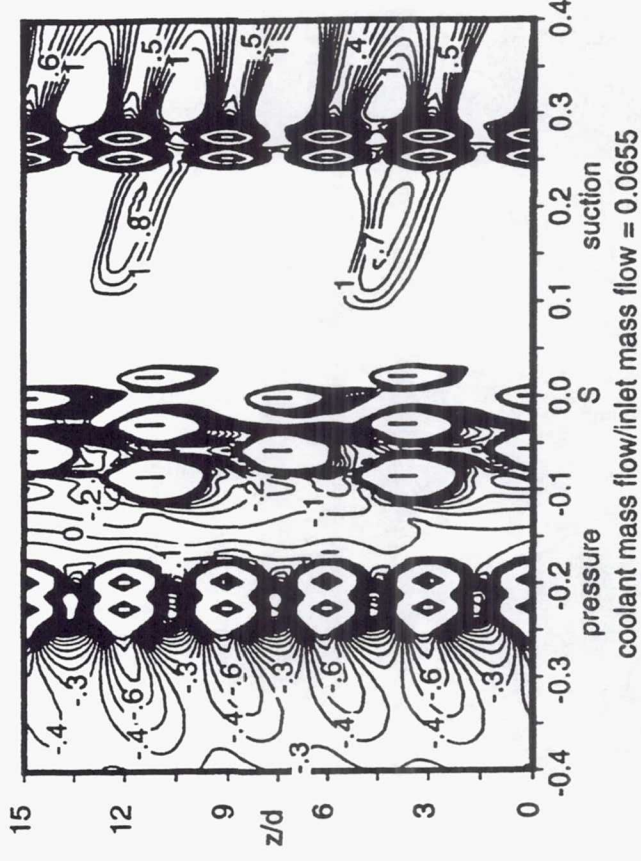
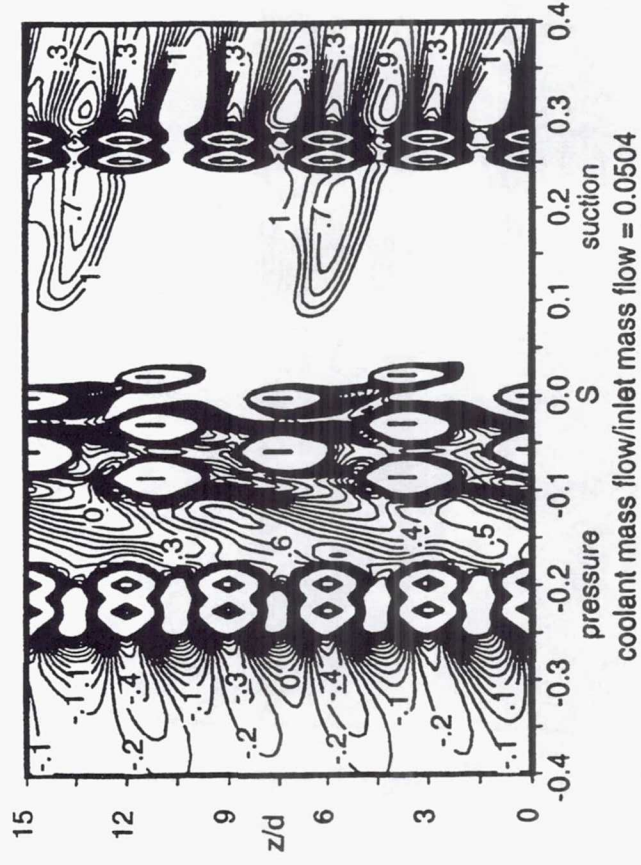
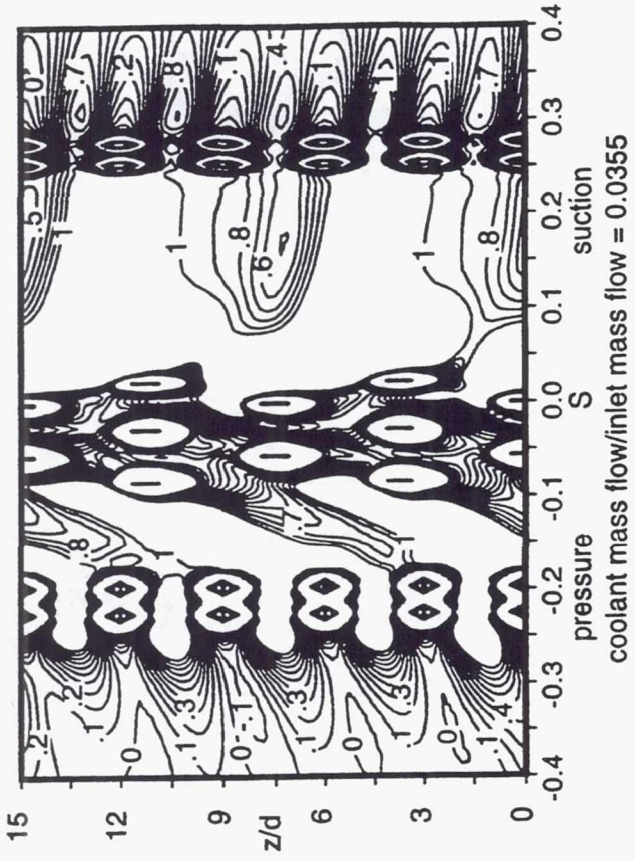
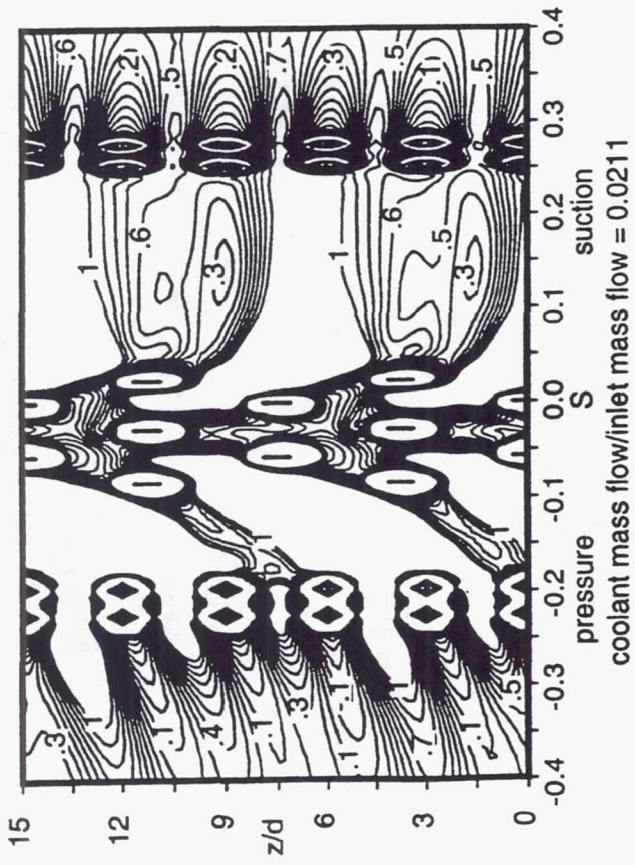


FIG. 11 NORMALIZED HEAT TRANSFER COEFFICIENT (h/h_0) CONTOURS ON THE C3X VANE SURFACE WHEN $P/d = 7.5$.

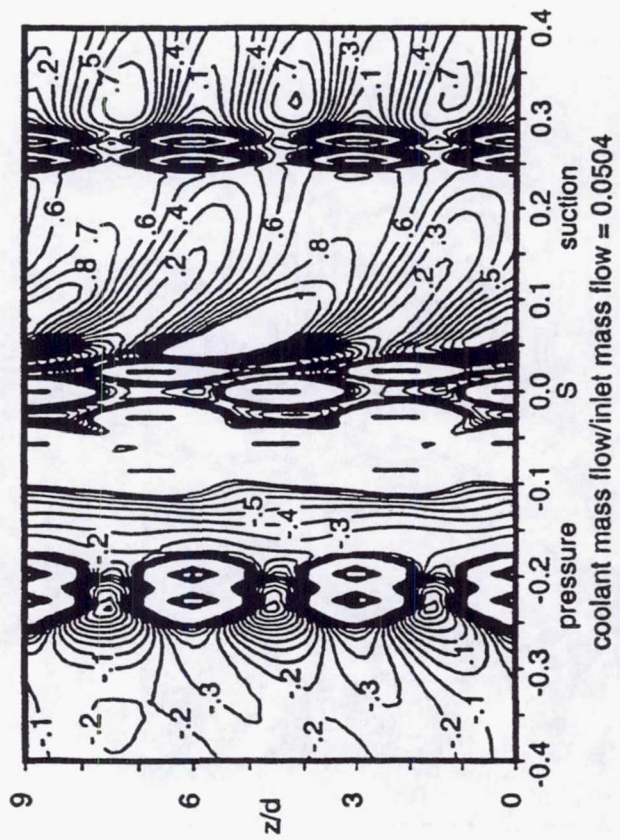
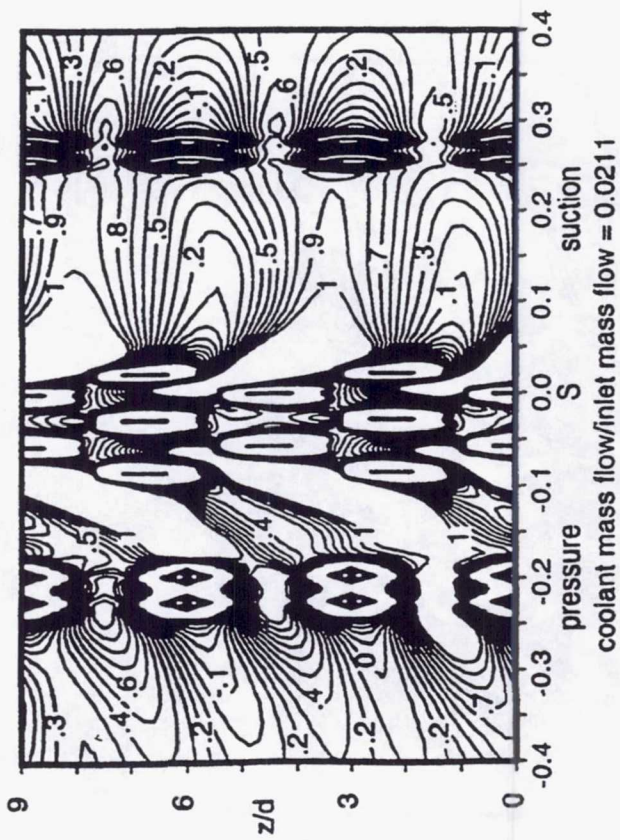
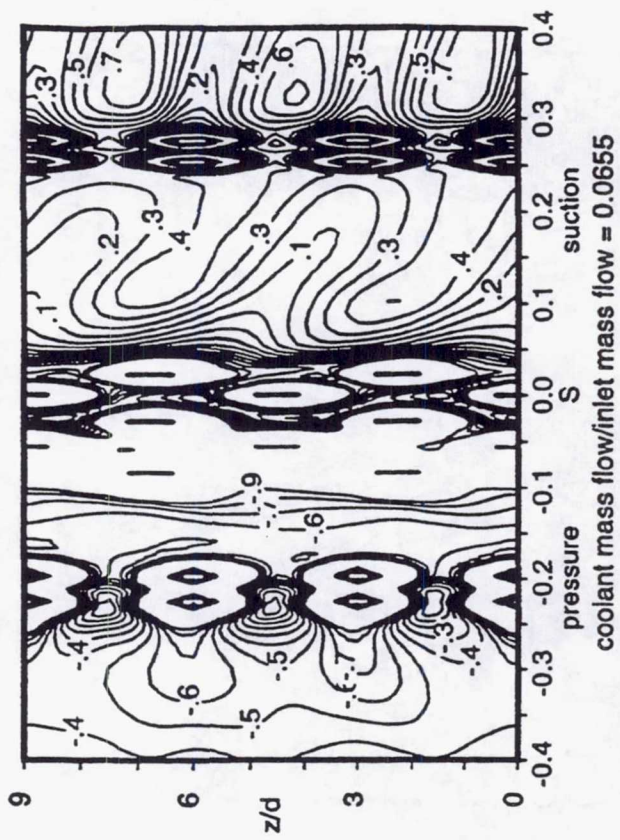
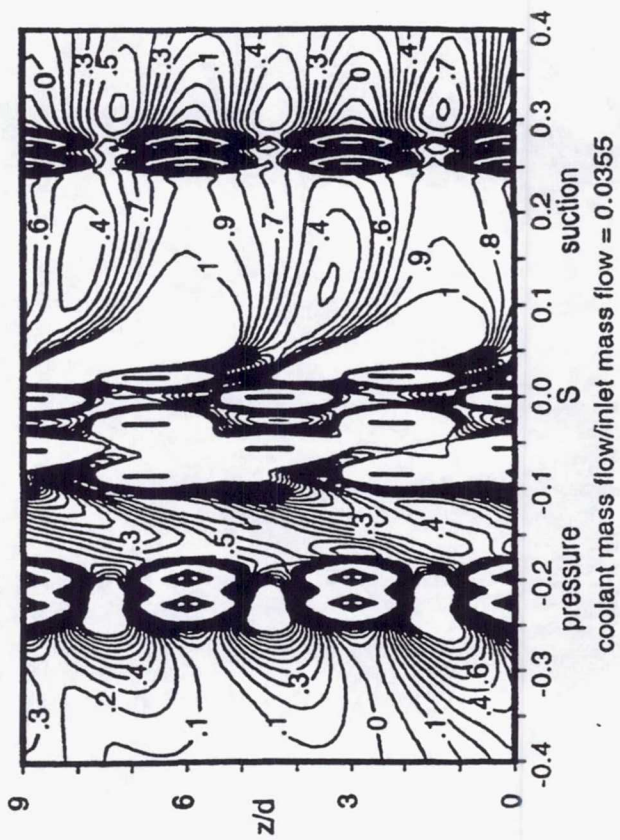


FIG. 12 NORMALIZED HEAT TRANSFER COEFFICIENT (h/h_0) CONTOURS ON THE C3X VANE SURFACE WHEN $P/d = 4.5$.

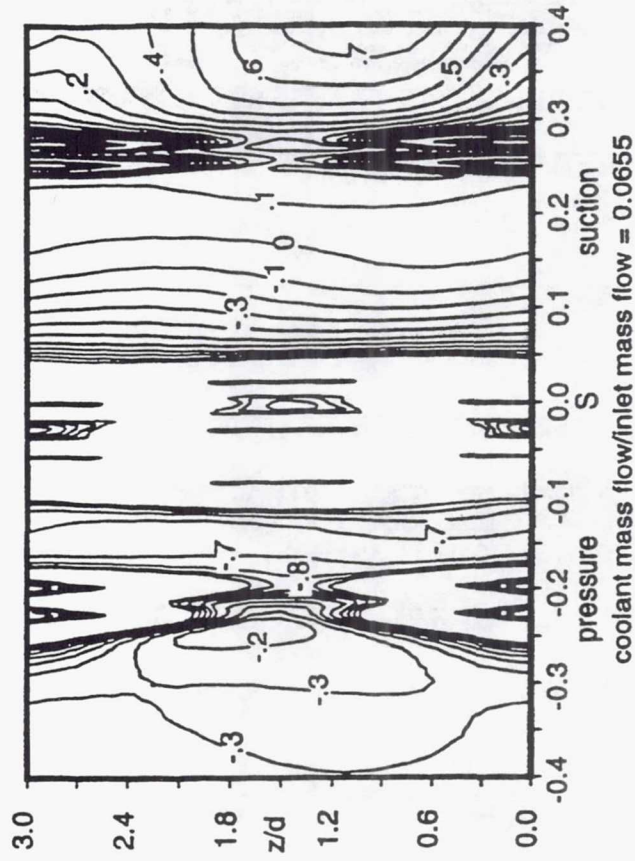
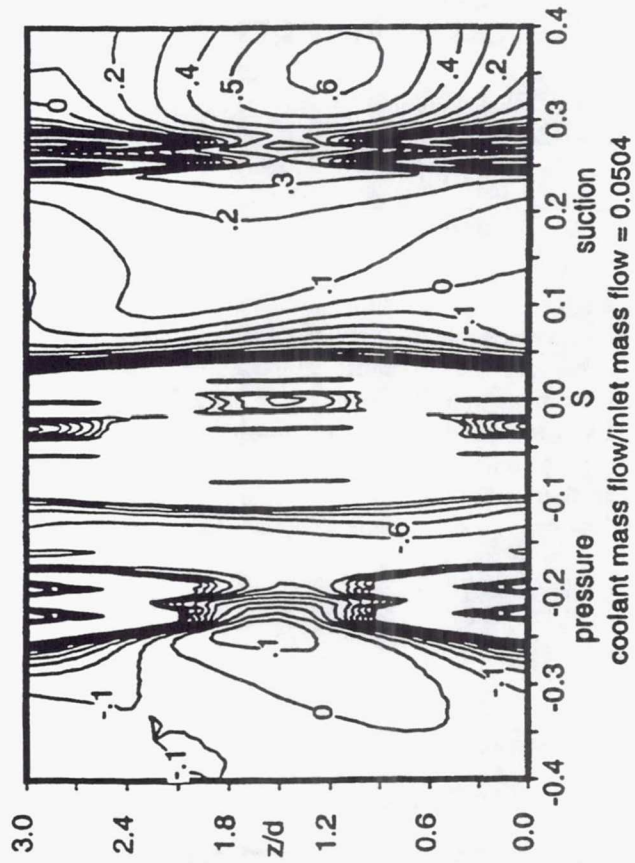
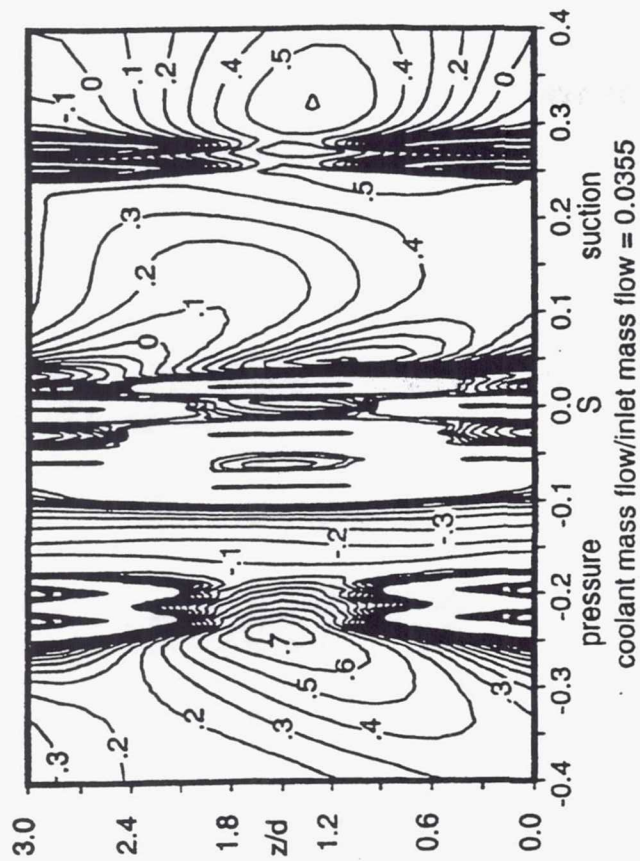
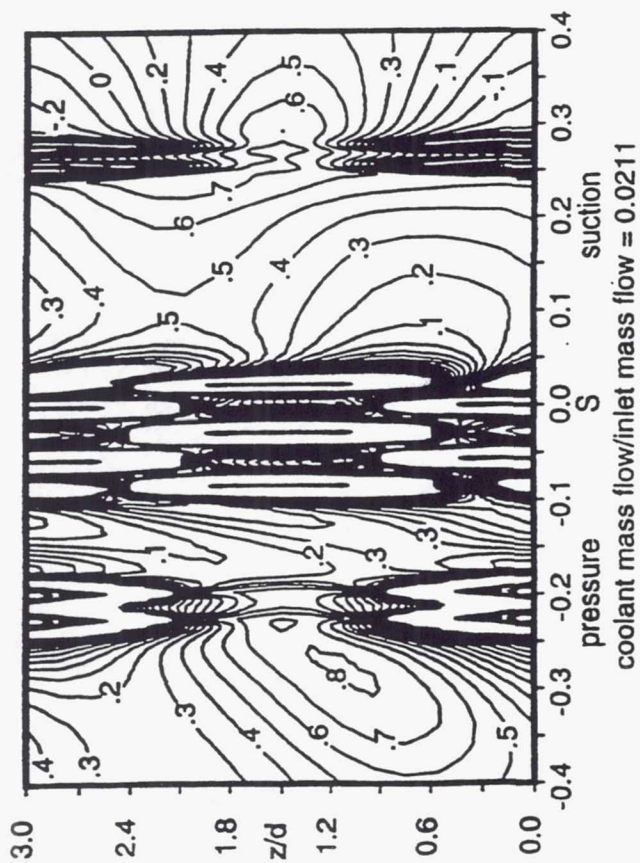


FIG. 13 NORMALIZED HEAT TRANSFER COEFFICIENT (h/h_0) CONTOURS ON THE C3X VANE SURFACE WHEN $P/d = 3.0$.

REPORT DOCUMENTATION PAGE

Form Approved
OMB No. 0704-0188

Public reporting burden for this collection of information is estimated to average 1 hour per response, including the time for reviewing instructions, searching existing data sources, gathering and maintaining the data needed, and completing and reviewing the collection of information. Send comments regarding this burden estimate or any other aspect of this collection of information, including suggestions for reducing this burden, to Washington Headquarters Services, Directorate for Information Operations and Reports, 1215 Jefferson Davis Highway, Suite 1204, Arlington, VA 22202-4302, and to the Office of Management and Budget, Paperwork Reduction Project (0704-0188), Washington, DC 20503.

1. AGENCY USE ONLY (Leave blank)	2. REPORT DATE June 1995	3. REPORT TYPE AND DATES COVERED Technical Memorandum	
4. TITLE AND SUBTITLE Leading Edge Film Cooling Effects on Turbine Blade Heat Transfer		5. FUNDING NUMBERS WU-505-62-52	
6. AUTHOR(S) Vijay K. Garg and Raymond E. Gaugler		7. PERFORMING ORGANIZATION NAME(S) AND ADDRESS(ES) National Aeronautics and Space Administration Lewis Research Center Cleveland, Ohio 44135-3191	
8. PERFORMING ORGANIZATION REPORT NUMBER E-9705		9. SPONSORING/MONITORING AGENCY NAME(S) AND ADDRESS(ES) National Aeronautics and Space Administration Washington, D.C. 20546-0001	
10. SPONSORING/MONITORING AGENCY REPORT NUMBER NASA TM-106955		11. SUPPLEMENTARY NOTES Prepared for the 40th Gas Turbine and Aeroengine Congress and Exposition sponsored by the American Society of Mechanical Engineers, Houston, Texas, June 5-8, 1995. Vijay K. Garg, AYT Corporation, Brook Park, Ohio 44142, and Raymond E. Gaugler, NASA Lewis Research Center. Responsible person, Raymond E. Gaugler, organization code 2640, (216) 433-5882.	
12a. DISTRIBUTION/AVAILABILITY STATEMENT Unclassified - Unlimited Subject Category 07 This publication is available from the NASA Center for Aerospace Information, (301) 621-0390.		12b. DISTRIBUTION CODE	
13. ABSTRACT (<i>Maximum 200 words</i>) An existing three-dimensional Navier-Stokes code, modified to include film cooling considerations, has been used to study the effect of spanwise pitch of shower-head holes and coolant to mainstream mass flow ratio on the adiabatic effectiveness and heat transfer coefficient on a film-cooled turbine vane. The mainstream is akin to that under real engine conditions with stagnation temperature = 1900 K and stagnation pressure = 3 MPa. It is found that with the coolant to mainstream mass flow ratio fixed, reducing P, the spanwise pitch for shower-head holes, from 7.5 d to 3.0 d, where d is the hole diameter, increases the average effectiveness considerably over the blade surface. However, when P/d = 7.5, increasing the coolant mass flow increases the effectiveness on the pressure surface but reduces it on the suction surface due to coolant jet lift-off. For P/d = 4.5 or 3.0, such an anomaly does not occur within the range of coolant to mainstream mass flow ratios analyzed. In all cases, adiabatic effectiveness and heat transfer coefficient are highly three-dimensional.			
14. SUBJECT TERMS Film cooling; Turbine; Heat transfer		15. NUMBER OF PAGES 19	
17. SECURITY CLASSIFICATION OF REPORT Unclassified		16. PRICE CODE A03	
18. SECURITY CLASSIFICATION OF THIS PAGE Unclassified	19. SECURITY CLASSIFICATION OF ABSTRACT Unclassified	20. LIMITATION OF ABSTRACT	